Published in final edited form as:
Dent Mater. 2012 July ; 28(7): 792–800. doi:10.1016/j.dental.2012.04.004.

Imaging *in vivo* secondary caries and *ex vivo* dental biofilms using cross-polarization optical coherence tomography

Pat Lenton[1], **Joel Rudney**[2], **Ruoqiong Chen**[2], **Alex Fok**[3], **Conrado Aparicio**[3], and **Robert S. Jones**[1,*]

[1]Department of Developmental and Surgical Sciences, University of Minnesota, 515 Delaware Street, Minneapolis, MN, 55455 USA

[2]Department of Diagnostic and Biological Sciences, University of Minnesota, 515 Delaware Street, Minneapolis, MN, 55455 USA

[3]Department of Restorative Sciences, University of Minnesota, 515 Delaware Street, Minneapolis, MN, 55455 USA

Abstract

Objectives—Conventional diagnostic methods frequently detect only late stage enamel demineralization under composite resin restorations. The objective of this study is to examine the subsurface tooth-composite interface and to assess for the presence of secondary caries in pediatric patients using a novel Optical Coherence Tomography System with an intraoral probe.

Methods—A newly designed intraoral cross polarization swept source optical coherence tomography (CP-OCT) imaging system was used to examine the integrity of the enamel-composite interfaces in vivo. Twenty two pediatric subjects were recruited with either recently placed or long standing composite restorations in their primary teeth. To better understand how bacterial biofilms cause demineralization at the interface, we also used the intraoral CP-OCT system to assess ex vivo bacterial biofilm growth on dental composites.

Results—As a positive control, cavitated secondary carious interfaces showed a 18.2 dB increase ($p<0.001$), or over 1-2 orders of magnitude higher, scattering than interfaces associated with recently placed composite restorations. Several long standing composite restorations, which appeared clinically sound, had a marked increase in scattering than recently placed restorations. This suggests the ability of CP-OCT to assess interfacial degradation such as early secondary caries prior to cavitation. CP-OCT was also able to image ex vivo biofilms on dental composites and assess their thickness.

Significance—This paper shows that CP-OCT imaging using a beam splitter based design can examine the subsurface interface of dental composites in human subjects. Furthermore, the probe dimensions and acquisition speed of the CP-OCT system allowed for analysis of caries development in children.

*Corresponding Author: Division of Pediatric Dentistry, School of Dentistry, University of Minnesota, 6-150 Moos Health Science Tower, 515 Delaware Street S.E. Minneapolis, MN 55455, Phone: 651-600-6836, fax: 612-626-2900, rsjones@umn.edu.

1. Introduction

Acid producing bacteria from a dental biofilm (dental plaque) can demineralize dental enamel on the tooth's outer surface (incipient caries). Extensive demineralization is surgically removed by a dental drill and a biocompatible material, such as a resin composite, is placed. The outer interface between the dental material and the tooth's enamel is a site for re-colonization of the dental biofilm and ‘secondary demineralization’ (secondary caries) can often occur. Visual inspection, such as marginal staining, and tactile probing (e.g. dental explorer) that examines for the presence of surface cavitation, are unreliable in identifying early secondary caries prior to local enamel breakdown [1].

Optical coherence tomography (OCT) has seen broad applications in medicine [2-4] and biology and has also been used to image dental hard and soft tissue [5, 6]. Significant *ex vivo* research efforts have studied the use of OCT to detect early enamel demineralization and secondary caries [6-10]; however, more work is needed to determine if *in vivo* carious lesions can be detected under intraoral conditions by OCT system. OCT is a non-destructive imaging system that can utilize near-infrared (NIR) light to produce depth resolved images in dental enamel. NIR illumination, especially near 1310 nm, significantly improves the axial imaging depth over wavelengths in the visible range, since dental enamel has been shown to be nearly transparent to NIR light [11, 12]. Enamel demineralization highly scatters NIR light, and OCT measures this increased backscattering intensity [8]. The advancement of Fourier Domain acquisition methods such as Swept Source OCT [13-15], where the depth resolved signal is extracted by measuring the interference spectrum of the tissue signal, has made clinical applications of OCT more feasible. Swept Source OCT (SS-OCT) has increased the acquisition speed, providing near real-time video rate imaging, while improving the overall signal to noise ratio of the acquired images [16].

Previous studies have shown that Polarization Sensitive (PS)-OCT can detect and quantify surface demineralization by utilizing linearly polarized incident light and measuring the backscattered signal in two orthogonal axes [8, 17]. By using polarization-maintaining (pm) fiber in the system, one detector can measure the signal parallel to the incident polarization axis and a second detector can measure the signal in the perpendicular or cross polarization axis. The high refractive index of enamel (n=~1.63) and dental materials such as resin composite (n=~1.5) causes a significant surface reflection, which can confound the imaging. However, the reflected light maintains the incident polarization state. Therefore, by measuring the signal in the cross polarization axis, the surface reflection signal is reduced significantly depending on the degree of crosstalk within the pm fiber [18]. Since dental enamel is slightly birefringent (Δ n= -0.002) [19], a high degree of linear polarity of the incident light is maintained during the initial propagation into the subsurface tooth structure. Incipient and secondary demineralization initially affects the subsurface tooth structure before spreading deeper into the dental enamel or along the tooth-material interface. Demineralization causes an irregular arrangement of porosities in enamel with an increase in both the number and size of defects which are filled with water and organic material. An increase in both the irregularity [20] and pore size [21] cause a greater depolarization of the incident light. With demineralization causing higher degree of backscattering and depolarization than healthy tissue, the cross-polarization image provides excellent contrast between demineralized and healthy tooth structure [18].

In addition to contrasting demineralization with healthy sound enamel, cross polarization OCT imaging has the benefit of identifying demineralized tooth structure next to dental resin composites. OCT imaging of resin composites materials has been shown to be strongly influenced by the index of refraction differences between the resin and the reinforcement material [22]. Fortunately, in dentistry, esthetic qualities are enhanced when composite

compositions closely match the resin matrix (e.g. methacrylate-based or urethane-based, n = 1.40-1.48) with different combinations of glass fillers. For esthetic dental composites that do not possess titanium dioxide, the degree of scattering and depolarization is significantly less than demineralized tooth enamel [17]. This is especially important for clinician diagnosing demineralization adjacent to these materials (secondary caries).

This study investigates an *intraoral* cross polarization swept source OCT (CP-OCT) system with a Micro-Electro-Mechanical System (*MEMS*) Scanning Mirror. This system is designed to illuminate the sample with linearly polarized light and isolate the perpendicular axis through a polarizing beam splitter based design. This design isolates and measures only the cross polarization axis signal. This straight forward approach allows the clinician to read and assess a single image in order to diagnosis secondary caries adjacent to resin restorations. While detecting secondary caries is important to a clinician, there is also a growing need to understand how material properties affect the growth of dental biofilms in order to prevent secondary caries. The nature of complex multi-species biofilms at the enamel-tooth interface is close to unknown. In this paper, we also present our initial phase in using CP-OCT to assess the growth of *ex vivo* oral biofilm microcosms. These multi-species oral biofilm microcosms are derived from sampling dental plaque from pediatric dental subjects with a history of Early Childhood Caries and are at risk of developing secondary caries. By growing these oral biofilm microcosms rather than single species bacteria, we are creating a laboratory model system that better replicates the intraoral environment. The overall plan in using this model system is to understand the interaction between resin composites and oral biofilms and eventually elucidate the unique process that leads to secondary caries.

The aim of this paper is to illustrate that CP-OCT can be used to assess the enamel under the margins of composite restorations *in vivo* but can also be used to assess the growth of multi-species oral biofilm microcosms on these materials in our developing laboratory model.

2. Methods

2.1 Cross-Polarization Optical Coherence Tomography

A custom Cross-Polarization Swept Source OCT (CP-OCT) System with an Intraoral Probe (Figure 1) was developed (IVS-200-CPM, Santec Co. Komaki, Japan) for a pediatric dental application. The Swept Source system utilized a high swept rate (30 kHz) continuous wavelength scanning laser centered near 1310 nm with a bandwidth of 104 nm. Interferometric concepts of swept source OCT imaging are described elsewhere [23]. The interferometer component of the system (Figure 2) was housed in the intraoral probe body. This critical design was required so that the sample and reference arm paths experienced similar vibrations and significantly reduced the motion artifact caused from the device being used freehanded during intraoral imaging. The output beam from the swept source travels in single mode fiber and then was split to a sample and reference arm. In the sample arm, the output signal traveled through a collimator system and traveled through a polarizing beam splitter. The output wave was linearly polarized in the P-polarization state. Light then traveled through a fixed focusing lens (f=60) and was reflected onto a two axis tilt Micro-Electro-Mechanical System (*MEMS*) scanning mirror in the body of the probe. The *MEMS* mirror could collect B-scans (two dimensional images at 20 frames/second) in both an x and y direction. In order to accommodate the narrow spaces of the oral cavity, the linearly polarized output beam is reflected at the probe end to illuminate (~ 8 mW) the tissue sample. The backscattered signal from the tissue sample traveled back through the probe and the polarizing beam splitter. At this point, the S-polarization state (cross-polarization of the incident beam) was diverted to recombine with the reference signal. The signals from the sample and reference arms were recombined and measured by balanced detection. The

resulting interference pattern signal was recorded in time but can also be plotted in k-space (wavenumber) due to the time encoded wavenumber scanning of the output laser. The Fourier transform of this wavenumber spectrum produced the spatial information along the axial direction of the sample. The free space axial resolution for the source was experimentally measured to be 11 μm when a single reflective peak was measured at the -3 dB level. The dimensions of the probe was designed to be used freehanded and for a pediatric dental patient as young as 3 years old. Based on this constraint, the probe was designed with a fixed focal point lens. With the system focus fixed at 2.5 mm from the probe window, we choose a low numeric aperture (NA) design to maximize a Rayleigh range (depth of focus) of approximately 4 mm in order to accommodate imaging the complex tooth morphology. The trade off was an 80 μm lateral resolution ($1/e^2$) that was confirmed using a digital caliper.

2.2 Polarization Suppression Measurements

Parallel polarization suppression ratio of the CP-OCT system was measured by comparing two signal intensities with and without a quarter wave plate. An achromatic quarter wave plate was used (AHWP05M-1600, Thorlabs, Newton, NJ) with the fast axis aligned 45° to the linearly polarized incident beam. *With a quarter wave plate* (QWP) placed between the probe and a mirror, the illuminating linearly polarized light becomes circular polarized light and incident on the mirror. After reflecting from the mirror, the circular polarized light returns through the QWP where the light becomes orthogonally polarized (perpendicular axis or S-polarized) linear light. This S-polarized light is then reflected at the PBS and directed to recombine with the reference signal. By using the QWP, the total back reflected intensity was measured. *Without a quarter wave plate (normal design)*, unperturbed parallel polarized light was reflected back by the mirror to the incident path. In an ideal system, all parallel axis reflected light would not be directed to recombine with the reference arm. We measured the residual reflected light in the CP-OCT system that was detected by the balanced detectors.

2.3 Human Subjects and Image Analysis

Serial CP-OCT images of anterior and posterior composite resin restorations (fillings) in primary teeth were obtained from pediatric subjects. Pediatric Subjects (n=22) from an ongoing study examining oral biofilms associated with secondary caries are presented. One tooth was imaged per subject. Children were recruited from various clinics in the Minneapolis/Saint Paul metropolitan area and represented an ethnically diverse population. Particular efforts were made to recruit children with recently placed composite restorations in addition to those children who had restorations placed over 6 months prior to the study visit. Prior to enrollment, inform consent was obtained and human subject protection followed protocols approved by the Institutional Review Board at the University of Minnesota and by the National Institute for Health. The mean age of these patients was 8.5 years old. Only slight air drying (<3 seconds) or cotton roll drying was performed, prior to CP-OCT imaging, to remove any debris or excess pooling of saliva. The teeth were moist during imaging with no other isolation method utilized. Surface moisture and tissue hydration maintains the optical translucency of enamel [24]; therefore, enamel hydration improves the depth of CP-OCT imaging over excessive drying. A clinical disposable polyvinyl barrier covered the intraoral probe. To be included in the study, four thru twelve year old children had to have one primary tooth restored with an anterior or posterior resin composite. The exclusion criteria included children with significant medical conditions, chronic medication use leading to xerostomia, recent antibiotic use, and congential tooth anomalies. Each of the children enrolled had a chronic history of early dental decay and considered at risk of developing secondary caries under their restorations. A dental explorer was used to assess the enamel adjacent to the composite restorations (Class II or III). By

gently probing the adjacent enamel, the presence (tactile positive) or absence (tactile negative) of localized enamel cavitation was assessed for each restoration. The presence of tactile cavitation (tactile positive) was chosen as a definitive positive control since many visual signs (e.g. marginal staining) have been shown to be unreliable in determining the presence of secondary caries [1].

Raw CP-OCT images were image processed by a median filter to reduce the speckle noise inherent in OCT imaging. In addition, a small artifact produced by the internal reflections within the probe body was removed from a few images using an Exemplar based inpainting method [25]. This method was programmed in Matlab™ and Python™. For image analysis, the mean backscattered intensity of the subsurface enamel below the composite restoration up to 500 μm below the cavosurface margin was assessed using Matlab™. This was similar to the method employed previously for ex vivo evaluation [17]. The interface between the composite restoration and enamel was clearly demarcated due to the fundamental differences in the optical properties of the composite material and the underlying birefringent enamel [17].

2.3 *Ex vivo* Oral Biofilm Microcosms

In order to initially understand how intraoral bacteria colonize composite-tooth interfaces, we developed an *ex vivo* model to assess the attachment and growth of dental biofilms. The *ex vivo* oral biofilm model system was based on the CDC Biofilm Reactor (Biosurface Technologies Corporation, Bozeman, Montana). This biofilm reactor type allowed growth media (BMM, basal mucin medium) [26] to flow (~6.5 ml/min) through a vessel container that was stirred (125 rpm). Within the vessel container are circular coupons (e.g. resin composite discs, Filtek™ LS, 3M and hydroxyapatite, Clarkson Chromatography) mounted on rods. These discs acted as colonization sites for bacterial biofilms. In our design, these discs were disinfected by 70 % ethanol and then are pre-coated with sterilized (0.2 μm filter) diluted (Gibbon's buffer 1:1) saliva from pediatric subjects with a history of Early Childhood Caries. Next, fresh dental plaque (inoculums) sampled from tooth surfaces of matched subjects were added to the vessel. The inoculums within the vessel are initially incubated overnight (@37° C) in 350 ml of BMM. After incubation, media flow began and within a few hours the inoculums grew (@37° C) as a multispecies biofilm within the vessel and colonized the discs. Biofilms were allowed to grow on the hydroxyapatite and composite material for up to 2 days. We have confirmed, through DNA microarray analysis (HOMIM, Forsyth Institute)[27], that these colonizing multispecies biofilms preserve ~60% of the bacterial species in the original dental plaque sample. This confirmed that our approach more closely models the intraoral biofilm interaction with different surfaces than single species biofilms. CP-OCT imaging was done within 30 minutes after removal from the vessel with no histological preparation. Discs were also imaged using scanning electron microscopy (Hitachi TM-300) after the biofilms were fixed and stained with Alcian blue and osmium tetroxide, critical point dried, coated with palladium alloy.

3. Results

3.1 Polarization Suppression

Using the quarter wave plate, the CP-OCT system recombines all of the reflected and backscattered light from the mirror surface with the reference signal. The total intensity of the light from the single reflected point is recorded when using the quarter wave plate (Figure 3). Without the quarter wave plate, the normal design illuminated the sample with linearly polarized light (P-polarization state) and isolates the perpendicular axis light (S-polarization state) using a polarization beam splitter and a collimator system. A 31.4 dB

polarization suppression was measured indicating that over 99.9% of reflected light in the parallel axis does not recombine with the reference signal.

3.2 Intraoral CP-OCT Imaging of Dental Composites

Recently placed (within 6 months) restorations and those restorations with cavitated secondary carious lesions were used as negative and positive controls for this study, respectively. Figure 4 illustrates how the images of the enamel restoration margins of these two control groups are clearly differentiated. Figure 4 shows CP-OCT images of a recently placed composite, a composite placed over 6 months ago, and frank cavitated lesion. CP-OCT can detect demineralization by measuring the increase in scattering and depolarization of the NIR light by underlying enamel. With sound enamel adjacent to the interface, the underlying birefringent enamel does not significantly rotate the incident polarization state into the S-polarization. This is why CP-OCT images of sound tissue in Figure 4A appear so dark, while in Figure 4C the demineralization at the margin interface produces an intense backscattered signal.

Composite dental fillings (Figure 4) create various index of refraction mismatch boundaries that can be a source of a strong back reflected signal. These back reflected signals can potentially confound clinical evaluation in OCT imaging. By isolating the S-polarization signal, an accurate assessment of the marginal integrity of the enamel-composite interface was achieved (Figure 4). The cross-polarization image does allow the clinician to visualize birefringence banding that is evident when imaging sound dental enamel (Figure 4A). Dental composites are not birefringent and cause uniform scattering in depth, which allowed the material to be differentiated from the birefringent dental enamel (Fig 4A). Importantly, intact enamel-composite interfaces and sound underlying enamel show minimal scattering and depolarization.

To quantify scattering and depolarization in our CP-OCT images, we calculated the mean backscattering intensity of the enamel along the enamel-composite interface. Figure 5 shows that the mean backscattering intensity of the underlying enamel of a frank cavitated lesion was significantly higher (18.2 dB or over 1-2 orders of magnitude) than the underlying enamel from restorations recently placed ($p < 0.01$, Wilcoxon rank sum test). Figure 5 shows the standard deviations of the backscattered intensity measured in recently placed restorations and frank cavitated lesions for the reader's convenience; however, we used a more conservative non-parametric test for comparing the groups.

A majority of pediatric subjects with clinically sound composite restorations that were placed over 6 months prior to the study visit were shown to have very low mean backscattering intensity of the underlying enamel. The values measured in this group were similar to the values measured in our recently placed restoration group. Based on the minimal backscattering values, the underlying enamel was expected to be ‘sound’. However, there were three subjects in the group (Figure 5, boxed area) that had underlying enamel that dramatically backscattered and depolarized the incident light. The level of the backscattering intensity approached that of our positive control group with cavitated secondary caries. These three subjects had an average decayed and filled surface index of 15 and also had an average of 2.6 cavitated active lesions sites elsewhere in the mouth; these children would be classified as extremely high caries risk compared to the general population [28].

3.3 Assessing *Ex vivo* Oral Biofilm Microcosms

CP-OCT images of circular coupons of hydroxyapatite and resin composite were obtained before and after biofilm growth. The hydroxyapatite (HA) coupons have a similar chemical composition as dental tooth enamel. Despite a similarity in chemical composition, the HA

coupons do not have the organized crystal arrangement of dental enamel. The HA coupons are sintered and thus, produced from a compressed powder. The random arrangement of compressed power causes these coupons to highly scatter and depolarize the incident light. For the purposes of our CDC biofilm reactor, the HA discs are preformed for placement in our biofilm reactor, easily sterilizable, and are a model for bacterial tooth interaction. After oral biofilm microcosms were grown on the HA and resin composite coupons in the biofilm reactor, the CP-OCT images showed a difference in the uniformity of the biofilm growth and the overall height of the biofilm (Figure 6). SEM imaging of the coupons (Fig. 6) shows that these dental microcosms are thicker and more able to more uniformly grow on HA than the dental composite material (Filtek™ LS).

Discussion

The first significant result presented in this work was that the newly designed intraoral CP-OCT system had a polarization suppression of 31.4 dB and was quite efficient at isolating perpendicular axis light. The cross-polarization design of the system utilized polarizing beam splitters to accomplish this polarization suppression and did not rely on a more costly polarization maintaining fiber design. This is an important result considering the urgent need to lower OCT production cost, which is necessary for clinical adaptation. The polarization suppression allowed significant reduction of the surface reflection signal (P-polarization state) at the enamel or underlying tooth-composite interface (Figure 4). The CP-OCT presented in this study isolated and measured only the cross polarization axis signal after illuminating the sample with linearly polarized light.

The single cross polarization image produced was used to assess the backscattering intensity of the underlying enamel in primary tooth composite restorations. Another significant result in this study was obtaining CP-OCT images under intraoral conditions and on pediatric subjects. The MEMS scanning mirror in the probe and 30 kHz A-scan acquisition rate allowed images to be acquired at 20 frames per second. This frame rate not only was efficient at sampling multiple sections of the tooth but also allowed for freehanded acquisition with minimal motion artifact on pediatric subjects as young as 4 years old. Our cross sectional study design did not allow us to precisely know the exact composite brand that was used as a dental filling material for every subject. But we did observe that all tooth colored composites that were sampled in this study did not significantly depolarize or scatter the linearly polarized incident light. Most composite material scattered and depolarized the incident light to a similar degree as the surrounding enamel with the exception of the enamel birefringence effects. With the overall backscattering intensity of sound enamel being minimal, CP-OCT imaging along the material interface clearly demonstrates strong contrast between healthy (sound) versus demineralization tooth enamel.

This paper is in agreement with a previous publication that demonstrated the minimal effect of sound enamel under a composite material to alter the polarization state of the linearly polarized light [17]. Therefore, as linearly polarized light propagates through the composite-enamel interface a minimal signal in the cross polarization state is recorded by the CP-OCT images. Our work illustrates how restorations that were recently placed *in vivo* show a weak signal in the CP-OCT image. It is expected that minor phase retardation or polarization rotation caused by the sound enamel birefringence will produce some measurable but minimal alterations in the polarization state of the incident light. Conventional OCT, which is congruent to measuring incident linearly polarized light in the parallel axis plane [8, 17], has shown that the sound enamel under a resin composite system will produce a higher degree of backscattering/backreflection. This is explained by the index of refraction mismatch between the resin composite and the underlying sound enamel. The refractive index mismatch produces a specular reflection that is measured by Conventional OCT or the

Parallel axis image in a PS-OCT system. Gap formations [29] and porosities [30] in the composite resin or at the interface produce an even greater specular refection effect since these defects are likely filled with air or fluids where the refractive index mismatch is higher. Conventional OCT has the ability to detect these defects [31] and attempts have been made to measure the dimensions of these defects [29]; however, more work is needed to determine if gap formations can confound the ability to differentiate early *in vivo* demineralized enamel versus defects in the interface.

We are careful to point out that our cross polarization design may limit the ability to image interfacial defects that do not alter the polarization state of the linearly incident polarized light. Future studies with our design will need to address this fact, but we believe that this study adds to the evidence, especially under intraoral imaging conditions, that CP-OCT provides strong contrast between *in vivo* formed secondary carious lesions and sound enamel. For the purposes of a clinical decision to retreat the tooth, demineralization should be regarded as the most important criteria.

Using conventional detection methods, a dentist is faced with trying to assess micron level changes near the interface of a restoration with visible and tactile methods that overlook early secondary caries. The visible light photographs taken in Figure 4 illustrate the clinical difficulty in diagnosing early secondary caries with conventional methods. CP-OCT measured the scattering of early demineralization of the underlying enamel prior to cavitation (Figure 4B). Our *in vivo* results are comparable to a recent *ex vivo* cross polarization OCT study showing the higher overall reflectivity of artificially generated early secondary caries compared to that of sound underlying enamel [32]. Importantly, our study design relied on using recently placed restorations and cavitated lesions as our negative and positive controls, respectively. Based on human subject protections, we are not able to clinically validate through surgical intervention the ability of CP-OCT to detect early demineralization. This is because it is yet to be determined what degree of demineralization measured by CP-OCT requires surgical intervention, especially on teeth that will exfoliate in the near future. However, our primary tooth model allows us to collect exfoliated teeth over the course of the next 4 years to histologically validate our study results.

This study also demonstrated the ability of a CP-OCT system to image and to assess the heights of oral microcosm biofilms on hydroxyapatite and dental composite material. This is important as we begin to screen various dental composite materials for their effects on biofilm attachment and growth. Previous work in the area of biofilm assessment in laboratory models have shown that OCT can assess single species bacterial growth in a standard capillary flow-cell model [33]. However, a recent well designed assessment of oral bilofilm growth by OCT avoided imaging biofilms from normal incidence because of the surface reflection effect [34] . Since the magnitude of backscattering in normal OCT is dependent on the beam focus and depth of field, imaging biofilms at angles away from normal incidence can alter the overall assessment of the scattering of the biofilm. By measuring the vertical dimension of the biofilm, CP-OCT was able to compare biofilm growth heights and this was made easier by imaging at near normal incidence. SEM was not capable of measuring the height of the biofilms but is capable of much higher resolution than our CP-OCT images. SEM will continue to be a valuable tool in assessing biofilm attachment with the ability to morphologically characterize biofilm arrangement; however, SEM imaging requires histological preparation that does not preserve the vitality of the biofilm. CP-OCT is able to rapidly assess the overall biofilm attachment without histological preparation and has the potential to be used in longitudinal studies of biofilm attachment and growth.

4. Conclusion

This work demonstrated that CP-OCT imaging can be utilized to image and quantify the enamel integrity of enamel-composite restorations *in vivo*. By using a cross-polarization design, the underlying sound and carious enamel below the interfaces could be differentiated with high signal contrast. In addition, the high sweep rate of our system allowed freehanded acquisition that was important in imaging our pediatric subjects. Due to the high chronic dental decay rate in children, detecting early dental decay is important in order to minimize the trauma of replacing severe decay. Furthermore, detecting early secondary caries will allow us to better understand the nature of the biofilms at these interfaces and the clinical performance of restorative materials. We demonstrated that CP-OCT can also be valuable in assessing the growth of dental plaque microcosms in our laboratory model. This will allow future directions to optimize composite resin materials to prevent secondary caries.

Acknowledgments

This work was supported by NIH Grant 1R01DE021366-01, 3M Foundation Faculty Development Award, and the University of Minnesota. The authors would like to thank Ravi Chityala at U of M MSI for helping with image optimization.

References

1. Kidd EA, Beighton D. Prediction of secondary caries around tooth-colored restorations: a clinical and microbiological study. J Dent Res. 1996; 75(12):1942–6. [PubMed: 9033448]
2. Hee MR, et al. Optical coherence tomography for ophthalmic imaging- new technique. IEEE Engineering in medicine and biology magazine. 1995; 14(1):67–76.
3. Huang D, et al. Optical Coherence Tomography. Science. 1991; 254:1178–1181. [PubMed: 1957169]
4. Fujimoto JG, et al. High resolution in vivo intra-arterial imaging with optical coherence tomography. Heart. 1999; 82(2):128–33. [PubMed: 10409522]
5. Feldchtein FI, et al. In vivo OCT imaging of hard and soft tissue of the oral cavity. Optics Express. 1998; 3(3):239–251. [PubMed: 19384366]
6. Colston BW, et al. Dental OCT. Optics Express. 1998; 3(6):230–238. [PubMed: 19384365]
7. Baumgartner A, et al. Polarization-sensitive optical optical coherence tomography of dental structures. Caries Res. 2000; 34:59–69. [PubMed: 10601786]
8. Fried D, et al. Imaging caries lesions and lesion progression with polarization sensitive optical coherence tomography. J Biomed Optics. 2002; 7(4):618–627.
9. Amaechi BT, et al. Use of optical coherence tomography for assessment of dental caries: quantitative procedure. J Oral Rehabil. 2001; 28(12):1092–3. [PubMed: 11874506]
10. Ko AC, et al. Ex vivo detection and characterization of early dental caries by optical coherence tomography and Raman spectroscopy. Journal of Biomedical Optics. 2005; 10(3):031118. [PubMed: 16229643]
11. Fried D, et al. The nature of light scattering in dental enamel and dentin at visible and near-IR wavelengths. Appl Optics. 1995; 34(7):1278–1285.
12. Jones RS, et al. Near-infrared transillumination at 1310-nm for the imaging of early dental decay. Optics Express. 2003; 11(18):2259–2265. [PubMed: 19466117]
13. Chinn SR, Swanson EA, Fujimoto JG. Optical coherence tomography using a frequency-tunable optical source. Optics Letters. 1997; 22(5):340–342.
14. Golubovic B, et al. Optical frequency-domain reflectometry using rapid wavelength tuning of a Cr4+:forsterite laser. Optics Letters. 1997; 22(22):1704–1706. [PubMed: 18188341]
15. Lexer F, et al. Wavelength-tuning interferometry of intraocular distances. Applied Optics. 1997; 36(25):6548–6553. [PubMed: 18259516]
16. Choma M, et al. Sensitivity advantage of swept source and Fourier domain optical coherence tomography. Opt Express. 2003; 11(18):2183–2189. [PubMed: 19466106]

17. Jones RS, Staninec M, Fried D. Imaging artificial caries under composite sealants and restorations. J Biomed Opt. 2004; 9(6):1297–304. [PubMed: 15568951]

18. Jones RS, Fried D. Remineralization of enamel caries can decrease optical reflectivity. J Dent Res. 2006; 85(9):804–8. [PubMed: 16931861]

19. Theuns HM, et al. Birefringence and mineral content of the first stage of artificial carious lesion formation (a combined polarizing microscopic, microradiographic and scanning electron microscopic investigation). J Biol Buccale. 1982; 10(3):217–26. [PubMed: 6959998]

20. Egan W, Grusauskas J, Hallock H. Optical Depolarization Properties of Surfaces Illuminated by Coherent Light. Applied Optics. 1968; 7(8):1539–1534.

21. Schmitt JM, Xiang SH. Cross-polarized backscatter in optical coherence tomography of biological tissue. Optics Letters. 1998; 23(13):1060–1062. [PubMed: 18087429]

22. Dunkers JP, et al. Optical coherence tomography of glass reinforced polymer composites. Composites Part a-Applied Science and Manufacturing. 1999; 30(2):139–145.

23. Liu B, Brezinski ME. Theoretical and practical considerations on detection performance of time domain, Fourier domain, and swept source optical coherence tomography. Journal of Biomedical Optics. 2007; 12(4):044007–12. [PubMed: 17867811]

24. Brodbelt RH, et al. Translucency of human dental enamel. J Dent Res. 1981; 60(10):1749–53. [PubMed: 6944339]

25. Criminisi A, Perez P, Toyama K. Region filling and object removal by exemplar-based image inpainting. IEEE Transactions on Image Processing. 2004; 13(9):1200–1212. [PubMed: 15449582]

26. Wong L, Sissons CH. Human dental plaque microcosm biofilms: effect of nutrient variation on calcium phosphate deposition and growth. Arch Oral Biol. 2007; 52(3):280–9. [PubMed: 17045564]

27. Paster, B. Human Microbe Identification Microarray Protocols. 2008. Available from: http://mim.forsyth.org/docs/DNA%20Isolation%20Protocol.pdf

28. Oral Health in America: A Report of the Surgeon General-Executive Summary. U.S. Department of Health and Human Services, National Institute of Dental and Craniofacial Research, National Institutes of Health; Rockville, MD: 2000.

29. Bakhsh TA, et al. Non-invasive quantification of resin-dentin interfacial gaps using optical coherence tomography: Validation against confocal microscopy. Dent Mater. 2011; 27(9):915–25. [PubMed: 21665263]

30. Ishibashi K, et al. Swept-source optical coherence tomography as a new tool to evaluate defects of resin-based composite restorations. Journal of Dentistry. 2011; 39(8):543–548. [PubMed: 21651956]

31. Sinescu C, et al. Quality assessment of dental treatments using en-face optical coherence tomography. 2008; 13:054065. SPIE.

32. Stahl, J., et al. Imaging of Secondary Caries With Polarization Sensitive Optical Coherence Tomography. 2010. p. 40AADR

33. Xi C, et al. High-resolution three-dimensional imaging of biofilm development using optical coherence tomography. 2006; 11:034001. SPIE.

34. Von Basum, G., et al. Comparison Between qPCR and OCT for Biofilm Quantification in AADR/IADR2011. San Diego, CA: p. 1287

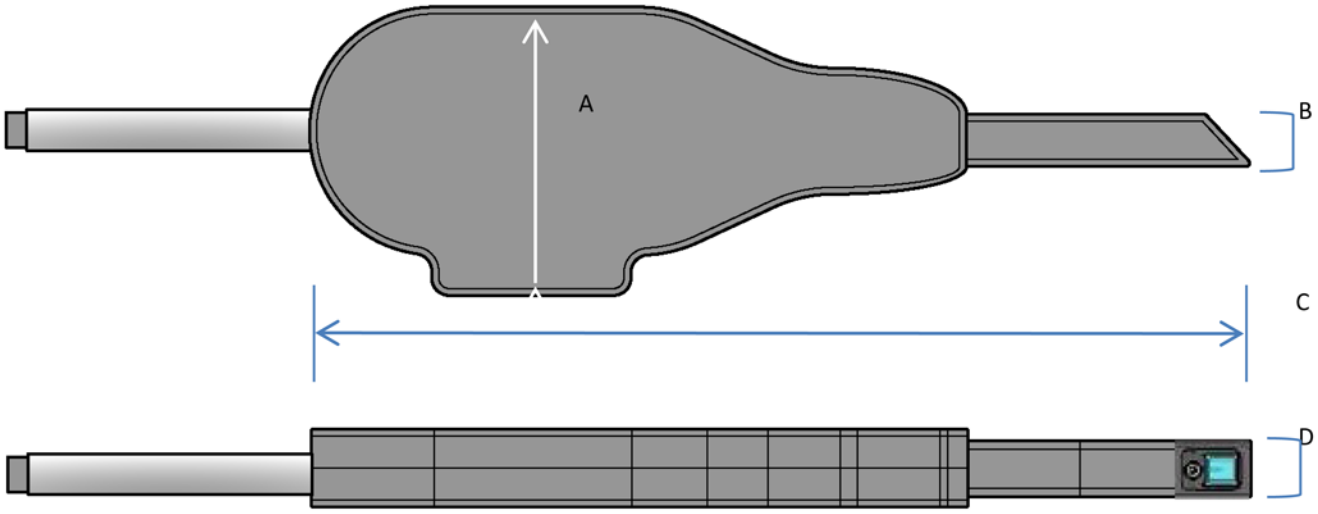

Figure 1.

Intraoral Probe with lateral and inferior views shown. A) The maximum height of the probe body is 82 mm. B) the height of the probe tip is 15 mm. C) the length of the entire probe is 265 mm. D) the width of the probe tip is 16 mm.

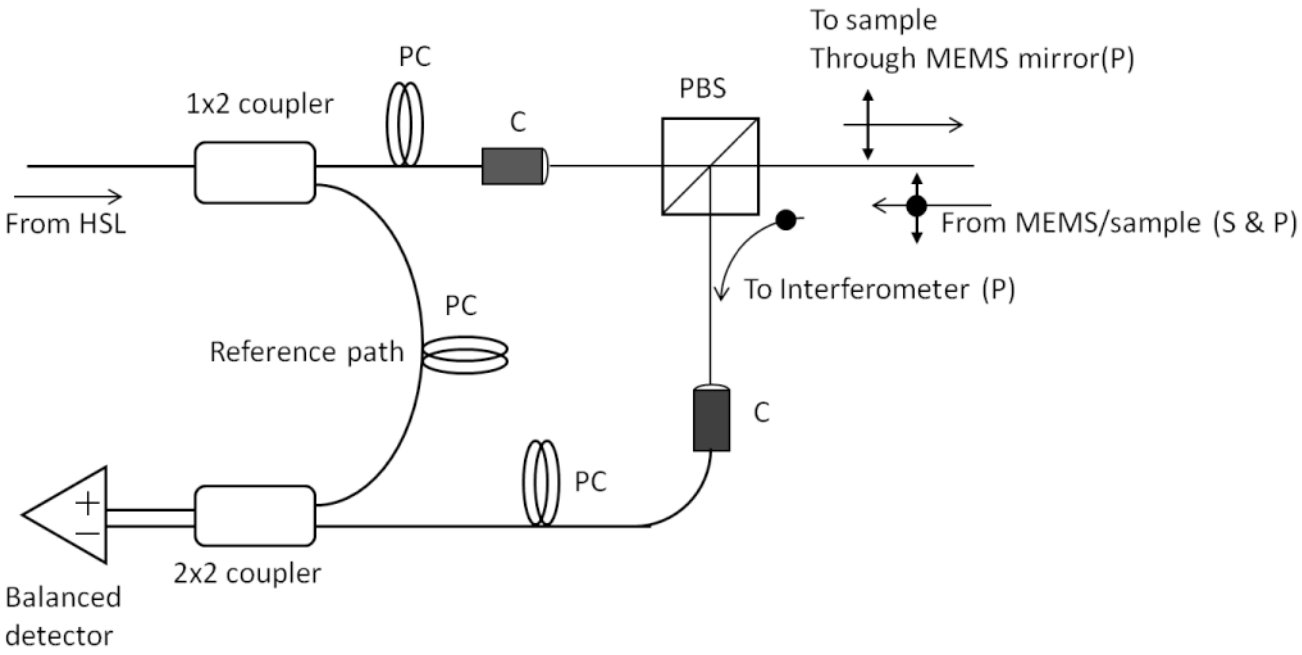

Figure 2.

Cross-Polarization OCT. Housed in the probe casing was a Mach-Zehnder type interferometer that used a polarization beam splitter (PBS) to illuminate a two axis tilt MEMS scanning mirror with linearly polarized light (P). Light from a swept source near infrared laser (HSL) was coupled into single mode fiber and then was split into a reference and sample arm. In the sample arm, a PBS isolated the cross polarization state (S) in the backscattered light. A collimator system (C) was used between the fiber and free space paths. In order to control the polarization states of the light in the reference and sample arms and produce an optimum interference pattern, polarization controllers (PC) were used. The interference signal was measured by two balanced detectors. The resulting electrical signal was then digitized by a high speed data acquisition board (DAQ) and image processed for reconstruction of the spatial information in the tooth sample.

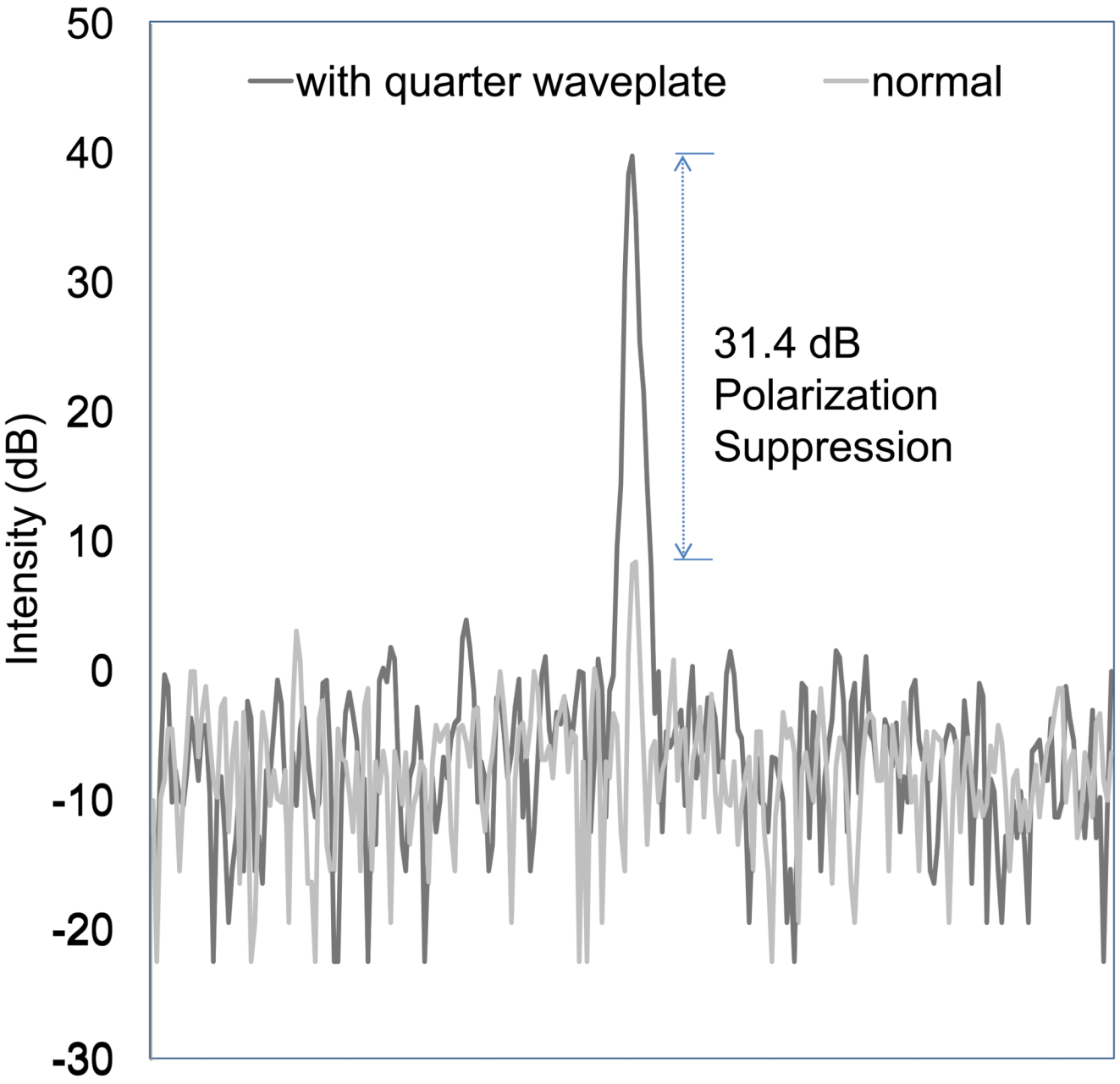

Figure 3.
Line profiles of a mirror surface. The x-axis is a function of depth and the y-axis shows the logarithmic intensity (dB) when the OCT probe was configured 1) normal-gray line or 2) with a quarter wave plate-black line. The two separate measurements are graphed together to illustrate the degree of polarization suppression, which is the difference between the two signals.

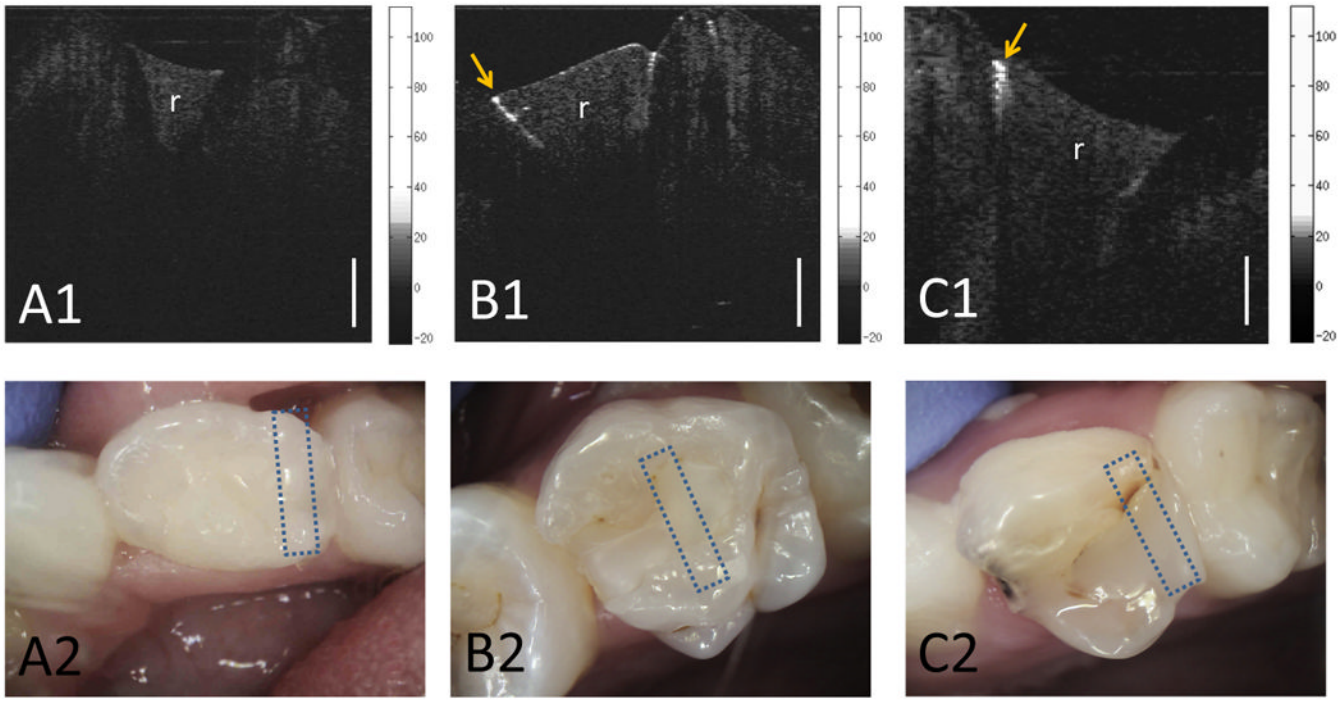

Figure 4.

A1) CP-OCT image and A2) intraoral photo of a resin composite filling (r) that was recently placed. B1) CP-OCT image and B2) intraoral photo of a resin composite filling (r) that has been in the mouth for well over 6 months and was clinically sound. The CP-OCT image shows high scattering of the underlying enamel below the restoration-tooth interface indicating an early failure of the restoration due to demineralization. C1) Positive control: CP-OCT image and C2) intraoral photo of a resin composite with cavitated secondary caries. The backscattered logarithmic intensity (dB) scales of the CP-OCT images are shown. The CP-OCT lateral scan distance was 5.2 mm. White scale bar is 1 mm of optical depth. Box areas shown on intraoral photos represent the area that was scanned with CP-OCT.

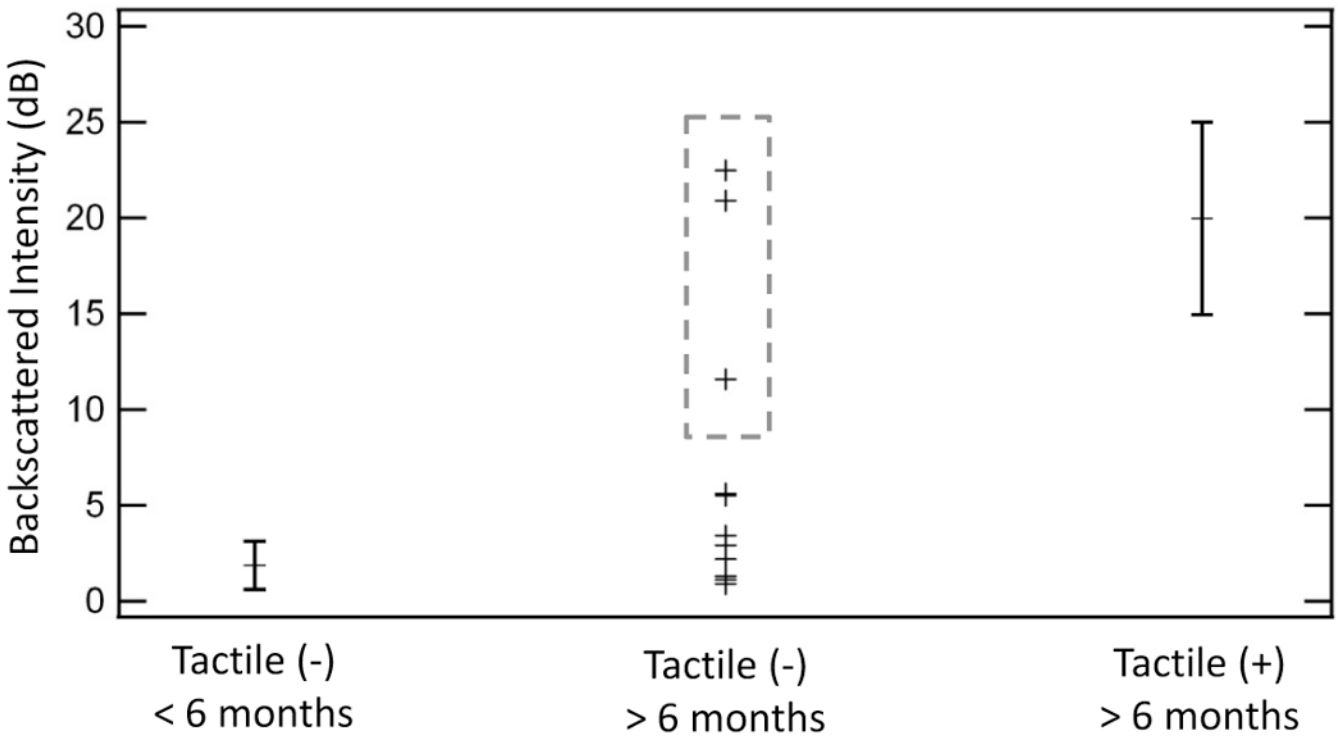

Figure 5.

Mean Backscattered Intensity of the subsurface enamel below the composite filling interface. Teeth (n=6) that were recently restored (< 6 months) with resin composites, which were assessed to be sound by tactile method, had underlying enamel with low backscattered intensity. Error bars represent the standard deviation. Cavitated secondary caries, which were tactile (+) and placed over 6 months ago, along the tooth-composite interface (n=5) had significantly higher ($p < 0.01$) backscattering intensity than restorations that were recently placed. A majority of the tactile sound composites (n=11), which were restored greater than 6 months ago, showed low enamel backscattering along the subsurface interface. However, several underlying interfaces (dotted box) showed a marked increase in enamel scattering than recently placed restorations. This suggests the ability of CP-OCT to assess early secondary caries prior to cavitation.

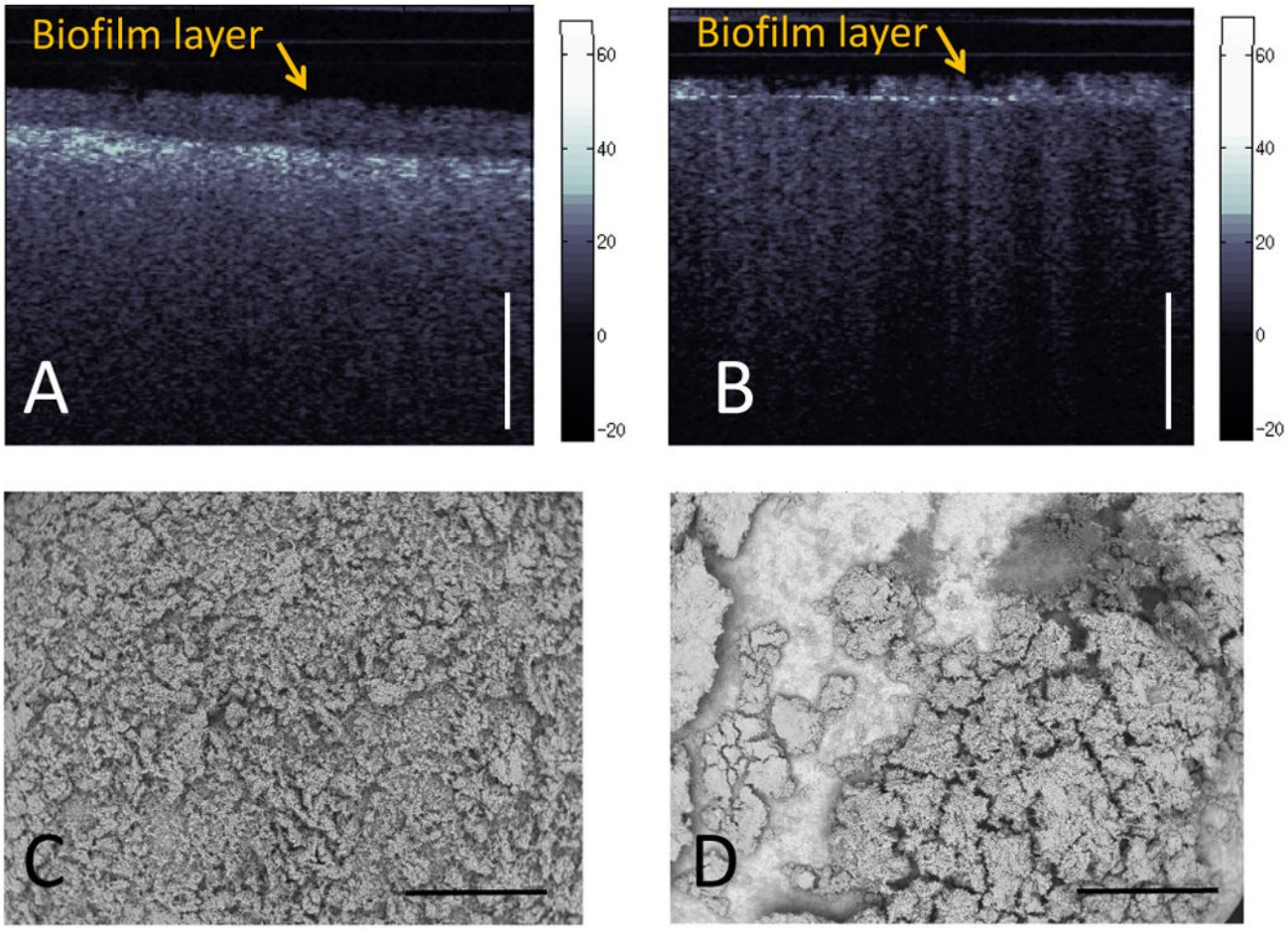

Figure 6.

A) CP-OCT images of oral biofilm microcosms growing on a hydroxyapatite disc. Using a refractive index estimate of 1.35, the biofilm height was 290 μm B) CP-OCT images of oral biofilm microcosms growing on a resin composite disc. False color scale of backscattered intensity (dB) shown and scale bar is 1 mm of optical depth. C) SEM images (40X) of oral biofilm microcosms growing on a hydroxyapatite disc. D) SEM images (40X) of oral biofilm microcosms growing on a resin composite disc. Scale bar is 1 mm.